A TEMPLATE-TO-SLICE BLOCK MATCHING APPROACH FOR AUTOMATIC LOCALIZATION OF BRAIN IN FETAL MRI

Vahid Taimouri, Ali Gholipour, Clemente Velasco-Annis, Judy A. Estroff, Simon K. Warfield

Computational Radiology Laboratory, Department of Radiology, Boston Children's Hospital
Harvard Medical School, Boston, Massachusetts, USA

ABSTRACT

To enhance post-acquisition processing of fetal brain MRI we have developed a template-to-slice block matching technique that matches a spatiotemporal (4D) atlas of the fetal brain to the corresponding section of the brain in each 2D fetal MRI scan. As compared to the recent studies which used feature based approaches for fetal brain localization, we propose a template matching approach that registers the template to each slice of the brain in 3D. In addition to brain localization, this novel technique registers the template to each fetal MRI scan thus is useful for slice-level motion correction, brain segmentation, and reconstruction. In this paper we describe the details of our algorithm and report statistical analysis of the accuracy of localization and registration. We examined the algorithm on 366 scans obtained from fetal MRI of 30 subjects and used a 4D MRI atlas of the fetal brain as template. Our results show 94% success rate in brain localization, and 73% successful matching, with a median localization error of 6.45 mm for all scans, and median target registration error of 4.2 mm for successfully localized scans. This algorithm can be used for automatic localization of fetal brain as the first step of fetal MRI analysis pipeline.

Index Terms— Fetal MRI, brain localization, template matching, registration, block matching.

1. INTRODUCTION

In-vivo fetal brain MRI analysis has accelerated in recent years mainly due to the advent of retrospective motion correction and volume reconstruction techniques [1-4]. Several groups have developed digital spatiotemporal MRI atlases of the fetal brain [5-7] and have used atlases for automatic segmentation, and volumetric and morphometric analysis [8, 9]. One of the potential applications of the developed spatiotemporal atlases of the fetal brain is to help improve fetal brain localization and reconstruction, and to automatize the entire fetal brain MRI analysis pipeline.

An important assumption in correcting inter-slice motion for fetal brain MRI reconstruction is that the motion of the fetal head is 3D rigid. Obviously this assumption is only valid for the fetal head and does not hold for the fetal and maternal organs such as the amniotic fluid, fetal hand and foot, and cord that surround the fetal head. Those organs can move non-rigidly in 3D and should be excluded from the fetal head motion correction and reconstruction process. Therefore, fetal head is often localized and extracted from images prior to volumetric fetal brain MRI reconstruction. The extraction of a region-of-interest around fetal head may be performed manually or automatically.

Automatic localization of the fetal brain in MRI has recently been addressed two groups [10, 11]. A two-stage Random Forest classifier was proposed in [10], and a Bag-of-Words model using SIFT features plus RANSAC for robust fitting was proposed in [11, 12]. As compared to these techniques, which focused on detecting a bounding box around the fetal brain, we propose a block matching technique to match (register) a spatiotemporal fetal brain MRI atlas to the fetal brain in each 2D fetal MRI slice.

While prior knowledge is encoded and used as features and scales based on gestational age in the previous studies, we use an age-matched template as prior and match it directly to each slice through an accelerated block matching approach. The immediate outcome of our novel template-to-slice block matching technique is automatic fetal brain MRI localization (similar to the previous studies), but in addition, we achieve template-to-slice matching (i.e. alignment in 3D), which can be used to improve fetal brain MRI reconstruction and segmentation.

2. METHOD

This method aims at estimating a rigid transformation to align a template (an age-matched fetal brain MRI template) to fetal brain MRI scans. We formulate our problem as a block matching algorithm in which the similarity between each block, i.e. a whole 2D slice, extracted from the template and a query image (a fetal MRI slice) is maximized. However, as we do not have any prior knowledge about the position of the fetal head, the similarity is computed between each block in the template with all 2D blocks in the query image. Consequently the search space is large and the problem is computationally intensive.

To limit the search space, we break the rigid transformation model to rotation (θ) and translation (T) parts, and estimate the parameters of each part separately.

For each rotation angle, the translation parameters are estimated through our block-matching technique. Further, we take advantage of dimension reduction as detailed below to accelerate the estimation process. The algorithm involves three steps: 1) block extraction and dimension reduction, 2) block matching using expectation maximization (EM), and 3) calculation of final transform by maximizing similarity.

2.1. Block extraction and dimension reduction

By computing the Sum of Square Distances (SSD) between a 2D block (i) in a template image and a 2D block (j) in the query image we generate a similarity matrix as,

$$\pi_{ij} = \frac{\exp(-\mathrm{SSD}_{ij})}{\sum_k \exp(-\mathrm{SSD}_{ik})}$$

In order to accelerate the calculation of the similarity matrix, we project each block to a lower dimensional space through a random matrix based on the Johnson-Lindenstrauss Lemma [13]. However, SSD is not rotation invariant, we need to initially rotate the template image using a rotation matrix (θ), extract the 2D blocks from the template, and compute the similarity matrix $\mathbf{\Pi}^\theta$ for each rotation matrix. Note that the resolution of the rotation angle is 45°, which according to our experiments yields satisfying performance in terms of speed and fetal brain localization accuracy.

2.2. Expectation maximization for match detection

After applying initial rotation θ and calculation of the similarity matrix $\mathbf{\Pi}^\theta$, we estimate the translation in the next step. Due to the large search space, and the similarity of surrounding structures such as the amniotic fluid and uterus wall, a block in the query image with the highest similarity with the template block may not necessarily indicate the correct match. Therefore, we collect multiple blocks in the query image with high similarity to each template slice. Let $\mathbf{A}$ be a binary matrix illustrating the match between the blocks in two images [14], thus $\mathbf{E_A}[A_{ij}] = p(\mathbf{A}_{ij} = 1)$. We consider:

$$p(\mathbf{A} = A) = \prod_{ij} \left(p(\mathbf{A}_{ij} = 1) \right)^{A_{ij}}, \tag{1}$$

such that $p(\mathbf{A}_{ij} = 1) = \pi_{ij}^\theta$. Let s_i and m_j be two block centers in the template image ($\mathbf{S}$) and the query image ($\mathbf{M}$), respectively. The joint probability of $\mathbf{S}$ and $\mathbf{A}$ is,

$$p(\mathbf{S}, \mathbf{A}|\mathbf{M}, T^\theta) = \prod_{ij} \left(\pi_{ij}^\theta \, p(s_i|m_j, T^\theta) \right)^{A_{ij}}, \tag{2}$$

where T^θ is the translation transferring the template to the fetal brain in the image after initial rotation θ, $p(s_i|m_j, T^\theta)$ is the probability of $T^\theta \circ s_i$ being homologous to m_j. Assuming the template image blocks are independent,

$$p(\mathbf{S}|\mathbf{M}, T^\theta) = \prod_i \sum_j \pi_{ij}^\theta \, p(s_i|m_j, T^\theta), \tag{3}$$

Hence we can determine the a-posteriori probability of the matches $\mathbf{A}$ as,

$$p(\mathbf{A}|\mathbf{S}, \mathbf{M}, T^\theta) = \frac{p(\mathbf{S}, \mathbf{A}|\mathbf{M}, T^\theta)}{p(\mathbf{S}|\mathbf{M}, T^\theta)} \tag{4}$$

which illustrates the a-posteriori matches between the two blocks with respect to s_i and m_j, and the translation T^θ. Equations (1) and (4) lead to the following equation [14],

$$\mathbf{E_A}[A_{ij}|\mathbf{S}, \mathbf{M}, T^\theta] = p(A_{ij} = 1|\mathbf{S}, \mathbf{M}, T^\theta)$$

$$= \frac{\pi_{ij} \, p(s_i|m_j, T^\theta)}{\sum_k \pi_{ik} \, p(s_i|m_k, T^\theta)} \tag{5}$$

We initially set the translation T to zero, and iteratively update it to maximize the probability of the block in $\mathbf{S}$ being matched to the blocks in $\mathbf{M}$,

$$\arg \mathrm{Max}_{T^\theta} \, \mathbf{E_A} \left[\log \left(p(\mathbf{S}, A|\mathbf{M}, T^\theta) \right) \right]. \tag{6}$$

Considering a normalized Gaussian probability for $p(s_i|m_j, T^\theta)$,

$$\arg \underset{T^\theta}{\mathrm{Max}} \, \mathbf{E_A} \left[\log \left(p(\mathbf{S}, A|\mathbf{M}, T^\theta) \right) \right] =$$

$$\arg \min_{T^\theta} \sum_{ij} p(\mathbf{A}_{ij} = 1|\mathbf{S}, \mathbf{M}, T^\theta) \| T^\theta \circ s_i - m_j \|^2 \tag{7}$$

We iteratively update the matches through Eq. (5) and the translation in Eq. (7). Through iterations of the EM steps formulated here, weights are assigned to a set of blocks with highest similarity and are updated to find the best match.

2.3. Final transformation

Once we calculate the translation T, we apply the translation and the initial rotation to the template, and calculate the similarity between the transformed template and the fetal image. Last, we choose the transformation with the highest similarity value as the most probable transformation, that is,

$$\arg \max_{\theta, T^\theta} \mathrm{NCC}(T^\theta \circ \theta \circ \mathbf{S}, \mathbf{M}), \tag{8}$$

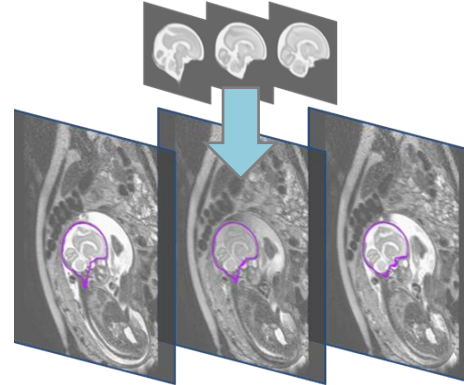where NCC is the normalized cross correlation (Fig. 1).

Fig. 1. In our template-to-slice algorithm, the 2D blocks of the template (top) are matched to the brain slices in the fetal MRI scan (bottom). The edge of the best match is shown as color overlay.
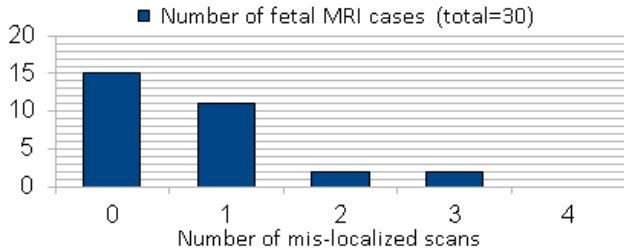
Fig. 2. Evaluation of the success rates of localization in the total number of 366 scans for 30 subjects. The graph shows the frequency distribution of mis-localized scans: in 15 subjects none of the scans was mis-localized and in none of the cases more than 3 scans were mis-localized. Total number of mis-localized scans was 21 (out of 366). This corresponds to 94% success rate.

3. EXPERIMENTAL RESULTS

We examined our algorithm on fetal MRI scans of 30 subjects. The gestation age (GA) of the fetuses at the time of MRI scans was between 27 to 36 weeks (mean=31, stdev=3). Imaging was performed on a 1.5T MRI scanner. For each subject multiple single shot fast spin echo (SSFSE) images were acquired with in-plane resolution of 1 to 1.25 mm, and slice thickness of 2 to 4 mm. The total number of SSFSE scans in our study was 366 which correspond to an average number of 12.2 scans per subject with standard deviation of 1.9. Each of these scans was used as a query image consisting of between 10 to 30 slices depending on the field-of-view and the size of the fetus in each study.

3.1. Localization accuracy

We used a spatiotemporal MRI atlas of the fetal brain as the template for brain matching [7]. We applied our matching algorithm and found bounding boxes around the fetal head in each scan (total number of 366 bounding boxes). We calculated the localization error (LE) in millimeter as the distance between the center of the computed bounding box and the bounding boxes defined by a trained observer (gold standard). Figure 2 shows the number of cases with 0 to 4 mis-localized scans. In 15 cases the brain was completely localized in all scans, and in none of the cases more than 3 scans (out of the average of 12.2 scans) was mis-localized. Figure 3(a) shows the boxplot of the localization error for 366 scans. The median of LE was 6.45 mm, which, as compared to the 240-300 mm field of view of the fetal MRI scans, and the sub-optimality of manually defined bounding boxes in the presence of inter-slice fetal motion, is remarkable. The boxplot analysis also detected 21 outliers which confirmed our qualitative evaluation in Figure 2. This indicates 94% success rate in fetal brain localization.

3.2. Registration accuracy

To calculate target registration error (TRE), we asked an expert to find 10 point landmarks separately on the matched template image and on the query image for each subject.

The landmarks were detected on axial, coronal, and sagittal slices chosen from a subset of scans (correctly localized according to the previous experiment) for each case. The landmarks included anterior commissure (AC), posterior commissure (PC), anterior point (AP), posterior point (PP), superior point (SP), and inferior point (IP). TRE was calculated in millimeter as the Euclidean distance between each pair of points on the matched template and each query image. Figure 3(b) shows the boxplot of the TRE in millimeters for the selected landmarks separately detected on the matched template image and each query image (Median of TRE = 4.2 mm). The boxplot analysis detected 100 outliers, which indicates 73% success rate in the fetus brain matching.
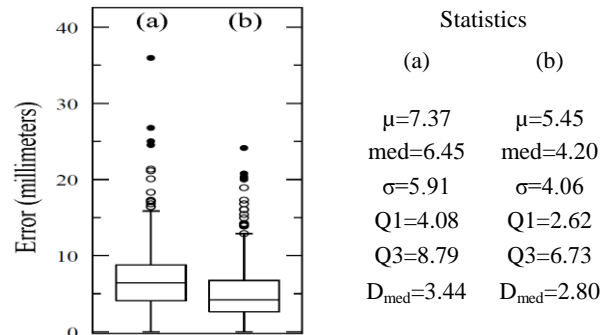

Statistics	
(a)	(b)
μ=7.37	μ=5.45
med=6.45	med=4.20
σ=5.91	σ=4.06
Q1=4.08	Q1=2.62
Q3=8.79	Q3=6.73
D_{med}=3.44	D_{med}=2.80

Fig. 3. Boxplot analysis and statistics of (a) the localization error, and (b) the target registration error computed for the landmarks detected manually on pairs of correctly matched template and query images for 30 fetuses (10 landmarks were detected on a set of slices for each fetus). The reported statistics include mean (μ), median (med), standard deviation (σ), first quartile (Q1), third quartile (Q3), and the mean absolute deviation from median (D_{med}) in millimeters.
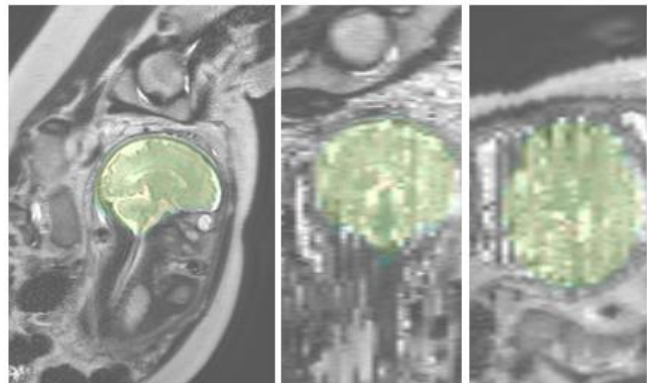

Fig. 4. Typical outcome of our template matching algorithm in a sagittal fetal MRI scan of a 34 week GA fetus with severe inter-slice motion artifacts (slice thickness = 4 mm); (a) sagittal view of the sagittal SSFSE scan, (b) coronal, and (c) axial views of the same scan that are disrupted by inter-slice motion artifacts, with the matched template image overlaid on the subject anatomy (in color). Our results show that, even under severe motion artifacts, our algorithm is capable of localizing the brain and matching the template to a good fraction of slices.

3.3. Robustness to the choice of template

We also examined the sensitivity of the algorithm to the use of templates that were one week younger than the subject. Our results showed that the median localization error increased from 6.45mm to 6.6mm, which shows that the algorithm is relatively robust to variations in anatomy and tolerates differences in maturation levels. Figure 4 shows an example outcome of our template-to-slice matching technique. Sagittal, coronal, and axial planes of the fetal MRI scans are shown in (a) to (c) along with the matched template scan as the color overlay image. Although excessive inter-slice motion affected the out-of-plane views, our algorithm was capable of localizing the brain via matching the template to the majority of high-quality slices.

4. CONCLUSION

We developed and examined a novel template-to-slice block matching approach to automatically find the brain in fetal MRI slices through matching a fetal brain MRI template. We first used this for brain localization and achieved a high success rate (94%) and a median localization accuracy of 6.45mm in extracting a bounding box around the fetal brain. Automatic localization eliminates the need for manual extraction of fetal brain region in volume reconstruction. We also evaluated the accuracy of template to slice matching by computing target registration error (TRE) between landmarks detected on the matched fetal brain template and the corresponding fetal MRI scans. We achieved success rate of 73% and median TRE of 4.2 mm which indicates accurate registration which may be used towards improved motion correction, slice-level fetal brain MRI segmentation, and reconstruction. These are the subject of ongoing work.

5. ACHNOWLEDGEMENTS

6. REFERENCES

[1] F. Rousseau, *et al.*, "Registration-based approach for reconstruction of high-resolution in utero fetal MR brain images," *Acad Radiol,* vol. 13, pp. 1072-81, Sep 2006.

[2] S. Jiang, *et al.*, "MRI of moving subjects using multislice snapshot images with volume reconstruction (SVR): application to fetal, neonatal, and adult brain studies," *IEEE Trans Med Imaging,* vol. 26, pp. 967-80, Jul 2007.

[3] A. Gholipour, J. A. Estroff, and S. K. Warfield, "Robust super-resolution volume reconstruction from slice acquisitions: application to fetal brain MRI," *IEEE Trans Med Imaging,* vol. 29, pp. 1739-58, Oct 2010.

[4] M. Kuklisova-Murgasova, *et al.*, "Reconstruction of fetal brain MRI with intensity matching and complete outlier removal," *Med Image Anal,* vol. 16, pp. 1550-64, Dec 2012.

[5] P. A. Habas, *et al.*, "A spatiotemporal atlas of MR intensity, tissue probability and shape of the fetal brain with application to segmentation," *Neuroimage,* vol. 53, pp. 460-70, Nov 1 2010.

[6] A. Serag, *et al.*, "Construction of a consistent high-definition spatio-temporal atlas of the developing brain using adaptive kernel regression," *Neuroimage,* vol. 59, pp. 2255-65, Feb 1 2012.

[7] A. Gholipour, *et al.*, "Construction of a Deformable Spatiotemporal MRI Atlas of the Fetal Brain: Evaluation of Similarity Metrics and Deformation Models," in *Medical Image Computing and Computer-Assisted Intervention – MICCAI 2014*. vol. 8674, P. Golland, N. Hata, C. Barillot, J. Hornegger, and R. Howe, Eds., ed: Springer International Publishing, 2014, pp. 292-299.

[8] J. A. Scott, *et al.*, "Volumetric and surface-based 3D MRI analyses of fetal isolated mild ventriculomegaly: brain morphometry in ventriculomegaly," *Brain Struct Funct,* vol. 218, pp. 645-55, May 2013.

[9] A. Gholipour, *et al.*, "Multi-atlas multi-shape segmentation of fetal brain MRI for volumetric and morphometric analysis of ventriculomegaly," *Neuroimage,* vol. 60, pp. 1819-31, Apr 15 2012.

[10] M. Ison, *et al.*, "Fully Automated Brain Extraction and Orientation in Raw Fetal MRI," in *Workshop on Paediatric and Perinatal Imaging, MICCAI*, pp. 17-24.

[11] K. Keraudren, *et al.*, "Localisation of the brain in fetal MRI using bundled SIFT features," *Med Image Comput Comput Assist Interv,* vol. 16, pp. 582-9, 2013.

[12] K. Keraudren, *et al.*, "Automated fetal brain segmentation from 2D MRI slices for motion correction," *Neuroimage,* vol. 101, pp. 633-43, Nov 1 2014.

[13] W. B. Johnson and J. Lindenstrauss, "Extensions of Lipschitz mappings into a Hilbert space," *Contemporary mathematics,* vol. 26, p. 1, 1984.

[14] S. Granger and X. Pennec, "Multi-scale EM-ICP: A fast and robust approach for surface registration," *Lecture notes in computer science,* pp. 418-432, 2002.